

## CHANGES OF INSTABILITY THRESHOLDS OF ROTOR DUE TO BEARING MISALIGNMENTS

Helmut Springer and Horst Ecker  
Technical University of Vienna  
Vienna, Austria

Edgar J. Gunter  
University of Virginia  
Charlottesville, Virginia 22901

In this paper the influence of bearing misalignment upon the dynamic characteristics of statically indeterminate rotor bearing systems is investigated. Both bearing loads and stability speed limits of a rotor may be changed significantly by magnitude and direction of bearing misalignment. The useful theory of short journal bearings is introduced and simple analytical expressions, governing the misalignment problem, are carried out. Polar plots for the bearing load capacities and stability maps, describing the speed limit in terms of misalignment, are presented. These plots can be used by the designer to estimate deviations between calculation and experimental data due to misalignment effects.

## INTRODUCTION

Bearing misalignment and initial shaft bow may considerably change the dynamic characteristics of a rotor bearing system. In general, bearing misalignment and shaft bow represent imperfections of a system with unknown amount which cannot be predicted exactly by the designer. Therefore, a qualitative analysis, investigating the influence of bow and misalignment upon vibration amplitudes, dynamic bearing loads, and stability, etc., of a rotor, might be useful. Also significant deviations between experimental data and theoretical calculations of a rotor bearing system may be caused by bearing misalignments, for example. In this case an error estimation between experiment and calculation, considering the above mentioned imperfections, is necessary.

It is well known from the literature that beside static and dynamic unbalance of a rotor a residual shaft bow may be considered as an additional external force that is exciting the rotor with constant amplitude independent of the speed. If a linearized (first order) analysis is applicable to a system then initial shaft bow and unbalance do not change the stability characteristics of the rotor. In other words, no interactions between self-excited shaft whirl and external excitation can be described by a linear approach; for example, see reference 1. Therefore, in this paper the response of unbalance and shaft bow is not considered, since, in a first order sense, it does not change the onset of instability of the rotor.

Gasch has shown in his paper, see reference 2, that in a statically indeterminate rotor bearing system the static bearing loads depend upon the speed of the shaft because of nonlinear hydrodynamic bearing characteristics. Nasuda and Hori, reference 3, investigated the influence of journal bearing misalignment upon the stability characteristics. They determined so-called "contour stability maps" for a two-mass and four-bearing rotor.

In this paper the theory of short journal bearings is used, see reference 4, in order to calculate bearing loads, bearing stiffness and damping coefficients, and stability thresholds of a flexible rotor in terms of bearing misalignment. Both, magnitude and direction of the misalignment vector of a bearing are varied and ranges of high and low sensitivity of the stability limit can be observed.

#### NOMENCLATURE

[A]	dynamical matrix (1/s <sup>2</sup> )	L	bearing length (m)
b	magnitude of initial shaft bow (m)	$\lambda$	misalignment attitude angle (direction of misalignment with respect to vertical x-axis) (rad)
$\beta$	phase angle of initial shaft bow (rad)	m	magnitude of misalignment (m)
C	radial bearing clearance (m)	$m_x, m_y$	misalignment components in x- and y-direction, resp. (m)
[C <sub>B</sub> ]	bearing damping matrix (Ns/m)	[M]	mass matrix (kg)
[C <sub>E</sub> ]	external damping matrix (Ns/m)	$\mu$	dynamic viscosity of bearing lubricant (Ns/m <sup>2</sup> )
[C <sub>I</sub> ]	internal damping matrix (Ns/m)	N <sup>+</sup>	stability speed limit (Hz)
$\epsilon$	bearing eccentricity to clearance ratio	$\omega$	angular speed of shaft (1/s)
$\eta$	horizontal shaft displacement to clearance ratio	$\psi$	shaft center attitude angle (rad)
{F <sub>O</sub> }	external static load (N)	R	radius of the shaft at a bearing station (m)
{F <sub>B</sub> }	dynamic bearing load (N)	S = $\frac{\mu\omega L^3 R}{4\pi C^2 F_{Bo}}$	Sommerfeld number
{F <sub>Bo</sub> }	static bearing load capacity (N)	$\sigma$	eigenvalue (1/s)
$\phi$	bearing load attitude angle (rad)	t	time (s)
[I]	identity matrix	{U}	unbalance vector (kgm)
[K <sub>B</sub> ]	bearing stiffness matrix (N/m)	W	total weight of the rotor (N)
[K <sub>I</sub> ]	stiffness matrix due to internal damping (N/m)	{z}	shaft displacement vector (m)
[K <sub>S</sub> ]	shaft stiffness matrix (N/m)	{u}	eigenvector
$\kappa$	misalignment to clearance ratio		
$\xi$	vertical shaft displacement to clearance ratio		

Subscripts

B bearing  
 f,l first and last bearing station, respectively  
 j station number ( $1 \leq j \leq n$ )  
 n total number of shaft stations  
 o static load conditions  
 x,y vertical and horizontal direction, respectively

Superscripts

T transposition of a matrix or column vector

Brackets

{ } column vector  
 [ ] matrix  
 ( ) function of

EQUATIONS OF MOTION

Various definitions of bearing misalignments can be introduced for a rotor-bearing system. For example, in figure 1, lateral displacements of the bearings are measured with respect to a line that is connecting the centers of the outer bearings (i.e. first and last bearing). Beside lateral bearing misalignment slope misalignment of the bearing axis may occur in practice but is neglected in this paper. Also slope deviations between shaft axis and bearing axis are not considered in this investigation. Therefore, at least three bearings have to be present in order to get a statically indeterminate system that exhibits misalignment effects.

Initial shaft bow, for example, can be measured in a "non-assembled" strain-free configuration of the shaft where shaft centers and bearing centers at the first and the last bearing station coincide, see figure 1. In general, for an n-stations shaft the lateral misalignment vector is defined as

$$\{m\} = \{0, \dots, 0, m_{f+1} \cos \lambda_{f+1}, \dots, m_{1-1} \cos \lambda_{1-1}, 0, \dots, 0\} \\ \{0, \dots, 0, m_{f+1} \sin \lambda_{f+1}, \dots, m_{1-1} \sin \lambda_{1-1}, 0, \dots, 0\}^T \quad (1)$$

The magnitude of misalignment  $m_j$  for a "no-bearing" station j is defined to zero. Initial shaft bow is given by

$$\{b(t)\} = \{b_1 \cos(\omega t + \beta_1), \dots, 0, \dots, b_j \cos(\omega t + \beta_j), \dots, 0, \dots, b_n \cos(\omega t + \beta_n)\} \\ \{b_1 \sin(\omega t + \beta_1), \dots, 0, \dots, b_j \sin(\omega t + \beta_j), \dots, 0, \dots, b_n \sin(\omega t + \beta_n)\}^T \quad (2)$$

in terms of the shaft rotational angle  $\omega t$ , see figure 1. If internal and external damping forces are considered and gyroscopic forces are neglected then the equations of motion of the rotor-bearing system can be written in the form

$$[M]\{\ddot{z}\} + [C_E + C_I]\{\dot{z}\} + [K_S + K_I]\{z\} = \\ = \{F_o\} + [K_S]\{b(t)\} + \omega^2\{U(t)\} + \{F_B(\{z-m\}, \{\dot{z}\}, \omega)\} \quad (3)$$

where  $\{z\} = \{x_1, \dots, x_n | y_1, \dots, y_n\}^T$  is a column vector containing lateral (vertical and horizontal) displacements of the shaft at  $n$  stations, see reference 1. A Taylor-expansion of equation (3) with respect to the nonlinear bearing forces  $\{F_B\}$  is convergent if the static preload  $\{F_0\}$  is sufficiently high compared with unbalance and shaft bow excitation forces. Under this assumption an expansion leads to

$$[K_S + K_I]\{z_0\} - \{F_{B0}(\{z_0 - m\}, \{0\}, \omega)\} - \{F_0\} = \{0\} \quad (4)$$

and

$$\begin{aligned} [M]\{\ddot{z}_1\} + [C_E + C_I + C_B(\{m\}, \omega)]\{\dot{z}_1\} + [K_S + K_I(\omega) + K_B(\{m\}, \omega)]\{z_1\} = \\ = [K_S]\{b(t)\} + \omega^2\{U(t)\} \end{aligned} \quad (5)$$

with  $\{z\} = \{z_0\} + \{z_1(t)\}$  being the "first order" solution of equation (3). The stationary part  $\{z_0\} = \{z_0(\{F_0\}, \{m\}, \omega)\}$  of this solution is evaluated from the nonlinear system equations (4), with  $\omega = \text{const.} \neq 0$  being the angular speed of the shaft. The stability of  $\{z_0\}$  is governed by the linear system of differential equations (5) with initial shaft bow and unbalance being set to zero.

Note that first order stiffness and damping characteristics of the bearings,  $[C_B]$  and  $[K_B]$  respectively, depend upon the stationary solution  $\{z_0(\{F_0\}, \{m\}, \omega)\}$ . Therefore, the rotor's stability limit depends upon bearing misalignment  $\{m\}$  and is not influenced by the shaft bow  $\{b\}$  as long as the above expansion converges.

## BEARING CHARACTERISTICS

### Static load capacity

The static load capacity  $\{F_{B0}\}$  of the bearings is evaluated by employing the theory of short journal bearings, see reference 4 and figure 2. For a single bearing, located at station  $j$ , the static bearing load components in the vertical  $x$ - and the horizontal  $y$ -direction can be written in the form

$$\begin{Bmatrix} F_{Box} \\ F_{Boy} \end{Bmatrix} = \frac{\omega(\mu L^3 R)}{2C^2} \begin{Bmatrix} \xi_{oj}^{-\kappa_j} \cos \lambda_j & | & -\eta_{oj} + \kappa_j \sin \lambda_j \\ \eta_{oj} - \kappa_j \sin \lambda_j & | & \xi_{oj}^{-\kappa_j} \cos \lambda_j \end{Bmatrix} \begin{Bmatrix} \frac{-2\varepsilon_{oj}}{(1-\varepsilon_{oj}^2)^2} \\ \frac{\pi}{2(1-\varepsilon_{oj}^2)^{3/2}} \end{Bmatrix} \quad (6)$$

where

$$\varepsilon_{oj} = \sqrt{(\xi_{oj}^{-\kappa_j} \cos \lambda_j)^2 + (\eta_{oj} - \kappa_j \sin \lambda_j)^2} \quad (7)$$

is the local bearing eccentricity ratio at station  $j$  and  $\xi_{oj} = x_{oj}/C_j$ ,  $\eta_{oj} = y_{oj}/C_j$ , and  $\kappa_j = m_j/C_j$  are local static shaft displacement and bearing misalignment to bearing clearance ratios, respectively. Substituting equation (6) for each bearing into

equation (4) yields a nonlinear system of relations to be solved numerically for the static displacement vector  $\{z_0\} = \{x_{01}, \dots, x_{0n} | y_{01}, \dots, y_{0n}\}^T$ .

### Bearing stiffness and damping characteristics

Once the stationary solution of the rotor at  $\omega = \text{const.} \neq 0$  is determined for a given misalignment  $\{m\}$ , local bearing stiffness and damping matrices can easily be evaluated for a bearing at station  $j$  from

$$[K_{Bj}] = \frac{\omega}{2} \left( \frac{\mu L^3 R}{C^3} \right)_j [T_j] \begin{bmatrix} \frac{4\epsilon_{oj}(1+\epsilon_{oj}^2)}{(1-\epsilon_{oj}^2)^3} & \frac{\pi}{2(1-\epsilon_{oj}^2)^{3/2}} \\ -\frac{\pi(1+2\epsilon_{oj}^2)}{2(1-\epsilon_{oj}^2)^{5/2}} & \frac{2\epsilon_{oj}}{(1-\epsilon_{oj}^2)^2} \end{bmatrix} [T_j]^T \quad (8)$$

and

$$[C_{Bj}] = \frac{1}{2} \left( \frac{\mu L^3 R}{C^3} \right)_j [T_j] \begin{bmatrix} \frac{\pi(1+2\epsilon_{oj}^2)}{(1-\epsilon_{oj}^2)^{5/2}} & \frac{-4\epsilon_{oj}}{(1-\epsilon_{oj}^2)^2} \\ \frac{-4\epsilon_{oj}}{(1-\epsilon_{oj}^2)^2} & \frac{\pi}{(1-\epsilon_{oj}^2)^{3/2}} \end{bmatrix} [T_j]^T \quad (9)$$

respectively, with  $\epsilon_{oj} \neq 0$  and

$$[T_j] = \frac{1}{\epsilon_{oj}} \begin{bmatrix} \xi_{oj}^{-\kappa_j} \cos \lambda_j & -\eta_{oj}^{+\kappa_j} \sin \lambda_j \\ \eta_{oj}^{-\kappa_j} \sin \lambda_j & \xi_{oj}^{-\kappa_j} \cos \lambda_j \end{bmatrix} \quad (10)$$

being an orthogonal transformation matrix between a local r-t-reference frame of the bearing  $j$  and the global x-y-system, see figure 2. As an example, in figure 3a and 3b, respectively, dimensionless first order stiffness and damping coefficients for the short journal bearing are shown in terms of the Sommerfeld number. The load attitude angle  $\phi$  is chosen to be zero in this example, i.e. the direction of the static load coincides with the global (vertical) x-axis. For any other arbitrary load direction equations (8) and (9) have to be applied.

## STABILITY

After substituting the local bearing stiffness and damping matrices into the global matrices of equation (5) the corresponding eigenvalue problem

$$[A - \sigma I] \{u\} = \{0\} \quad (11)$$

can be solved for  $\sigma$  as a function of the rotor angular speed  $\omega$  and the bearing misalignment vector  $\{m\}$ . The dynamical matrix  $[A]$  is of dimension  $2n \times 2n$  and is given by

$$[A(\{m\}, \omega)] = \left[ \begin{array}{c|c} [0] & [I] \\ \hline -[M]^{-1}[K_S + K_I(\omega)] & -[M]^{-1}[C_E + C_I] \\ -[M]^{-1}[K_B(\{m\}, \omega)] & -[M]^{-1}[C_B(\{m\}, \omega)] \end{array} \right] \quad (12)$$

### EXAMPLE

Figure 4 shows a symmetric five stations rotor with three short journal bearings and two major masses mounted on a flexible shaft. The data for this rotor are listed in Table 1. The center bearing of the system may be misaligned with respect to the outer bearings by  $m_x$  and  $m_y$  in a vertical and horizontal direction, respectively. The numerical calculations for this example were carried out on the main frame computer CDC-CYBER 170/730 of the Technical University of Vienna, Austria. The nonlinear equation solver ZSPOW and the eigenvalue solver EIGRF of the IMSL-computer library were used.

Figure 5 shows the static load ratio of the center bearing in terms of the shaft speed. The horizontal misalignment  $m_y$  is kept zero while the vertical misalignment  $m_x$  is varied. It can be seen that each curve in figure 5 approaches the stability threshold at a certain speed of the rotor. The bearing load gradient is high at low speeds and decreases with increasing speed. The stability threshold is increasing with increasing misalignment above  $12 \mu\text{m}$  and below  $-5 \mu\text{m}$  in this example. In general, the center bearing load ratio in figure 5 is increasing with increasing speed except within a small range of misalignments between  $(-30 \mu\text{m} \leq m_x \leq -15 \mu\text{m})$  at low speeds. A similar diagram can be drawn for the outer bearing load ratios. Note that these bearing load characteristics might change with changes in the shaft bending stiffness and the bearing clearances. Also, in practice, the misalignment attitude angle  $\lambda$  is unknown and different from zero. Therefore, the influence of both  $m_x \neq 0$  and  $m_y \neq 0$  upon bearing loads and stability limits has to be studied.

Figure 6 shows polar plots for the bearing load ratios with the rotor speed kept constant at  $N=200$  Hz. Curves of constant magnitudes of misalignment are drawn in a plane where the polar angle indicates the direction of misalignment (attitude angle  $\lambda$ ) and the radius is the bearing load ratio, i.e. at constant radii the bearing loads are constant and at constant polar angles the ratio  $m_y/m_x$  is constant. At zero misalignment the load ratios of both center and outer bearings are constant. Hence, the curves

$m=0$  represent circles with constant bearing loads. For increasing magnitudes of misalignment the bearing load ratios change substantially with the direction of misalignment  $\lambda$ . For example, if a misalignment of  $10\ \mu\text{m}$  is present in the system, (i.e. 40% of the center bearing clearance or  $1/24000$  of the outer bearing span) then the center bearing load ratio varies between 0.2 at  $\lambda=25^\circ$  and 1.09 at  $\lambda=225^\circ$ . A corresponding change for the outer bearing can be seen on the right hand side of figure 6.

It is to expect that for misalignment directions that cause low bearing loads in the system the stability speed limit of the rotor is decreased also. This can be observed from figure 7, showing a polar plot of the stability limits of the present rotor. The polar angle in this diagram again indicates the direction of misalignment  $\lambda$  while the radius now is the stability speed limit. Curves of constant misalignment magnitudes are drawn in the figure. For low misalignments up to  $m=12\ \mu\text{m}$  and for attitude angles of about  $\lambda=20^\circ$  and  $\lambda=220^\circ$  the stability limits tip down significantly. For example, if  $m=10\ \mu\text{m}$ , then the stability limit of the rotor changes between  $N^+=275\ \text{Hz}$  and  $N^+=365\ \text{Hz}$ . Within the ranges of ( $180^\circ \leq \lambda \leq 250^\circ$ ) and ( $0 \leq m \leq 12\ \mu\text{m}$ ) a high sensitivity of the stability speed limit with respect to the direction of misalignment can be observed.

Stability maps and polar plots as discussed above give a complete information to the designer and make it possible for him to estimate misalignment effects upon the stability thresholds and the bearing load capacities of a given rotor.

#### CONCLUSION

The theory of short journal bearings makes it possible to formulate the misalignment problem of statically indeterminate rotor bearing systems in a simple and easy manner. The numerical effort to carry out bearing loads and stability limits in terms of misalignment is comparatively low even for a multi-station rotor supported by a multi-bearing system. There are a number of good and reliable algorithms available in various computer libraries to solve the governing equations of the problem. Since magnitude and direction of bearing misalignment are never exactly known in a real system the above presented theory is sufficiently accurate for practical applications and can be used by the designer in order to make a good estimation on whether or not a certain amount of bearing misalignment might dynamically endanger or damage a rotating machinery. Also the above results may explain deviations between experimental data and predictions where misalignment effects were not included.

#### REFERENCES

1. Springer, H., Ecker, H., Gunter, E.J.: Nonlinear Unbalance Response and Stability Thresholds of a Warped Multimass Rotor in Misaligned Bearings. Proceedings of Third Int. Conf. on Vibrations in Rotating Machinery. The Inst. of Mech. Eng., London, 1984, p.499-506.
2. Gasch, R.: Berechnung der Lagerlasten mehrfach gleitgelagerter Rotoren unter Berücksichtigung des nichtlinearen Verhaltens des Ölfilms. Konstruktion, 22, 1970, p.229-235 (in German).



ORIGINAL PAGE IS  
OF POOR QUALITY

DIMENSIONLESS BEARING STIFFNESS AND DAMPING CHARACTERISTICS  
FOR THE SHORT JOURNAL BEARING  
(Load attitude angle  $\phi = 0^\circ$ )

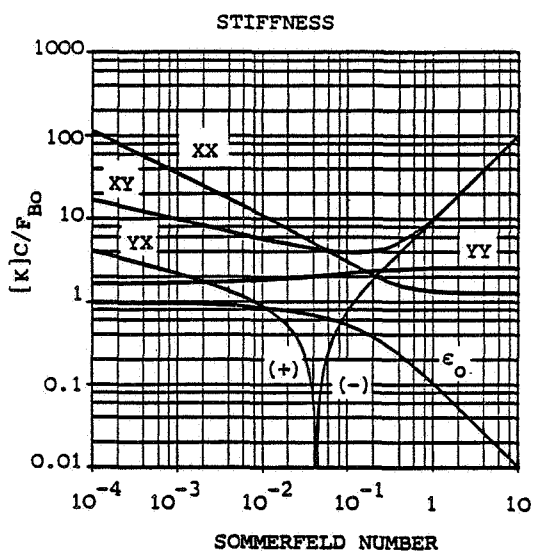


Figure 3a.

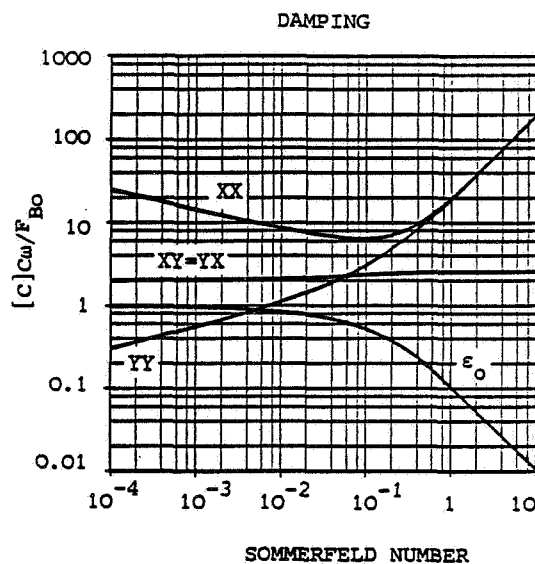


Figure 3b.

SYMMETRIC ROTOR BEARING SYSTEM  
WITH MISALIGNMENT

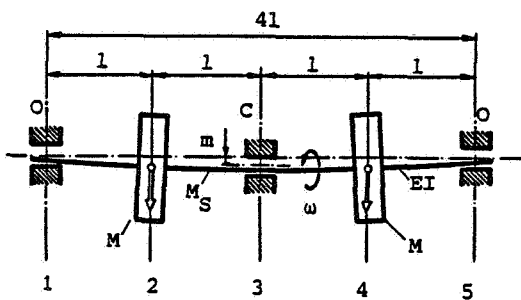


Figure 4.

CENTER BEARING LOAD RATIO VS.  
SHAFT SPEED FOR VARIOUS VERTICAL  
MISALIGNMENTS  $m_x$

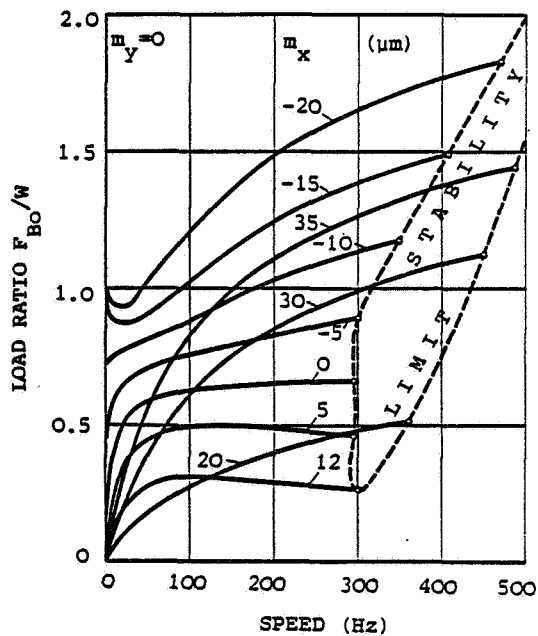


Figure 5.

BEARING LOAD RATIOS  $F_B/W$  IN TERMS OF MISALIGNMENT ATTITUDE  
 ANGLE  $\lambda$  AND MISALIGNMENT MAGNITUDE  $M$   
 (Rotor speed  $N = 200$  Hz)

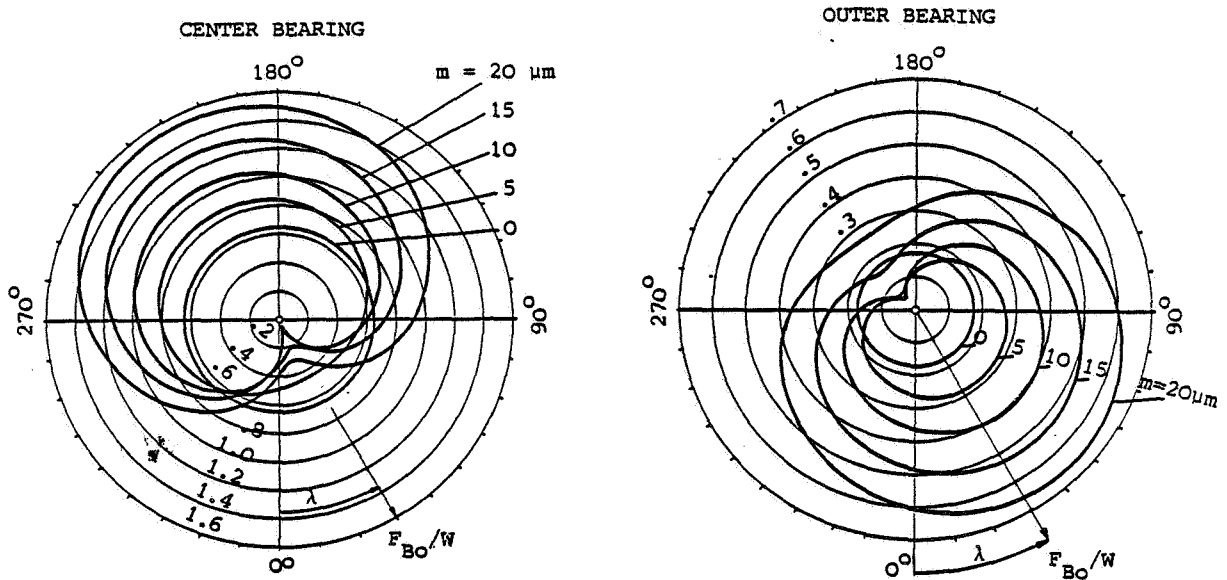


Figure 6.

STABILITY SPEED LIMITS  $N^+$  IN  
 TERMS OF MISALIGNMENT ATTITUDE  
 ANGLE  $\lambda$  AND MISALIGNMENT MAGNI-  
 TUDE  $M$

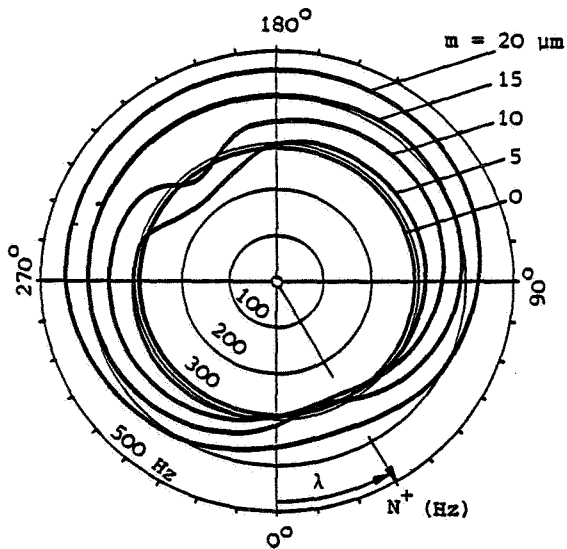


Figure 7.

DATA OF THE ROTOR BEARING SYSTEM  
 AS SHOWN IN FIGURE 4

Total mass of the rotor	16.8 kg	
Shaft bending stiffness	3350 Nm <sup>2</sup>	
Outer bearing span	240 mm	
BEARING DATA	CENTER	OUTER
Length	15 mm	7.5 mm
Diameter	25 mm	12.5 mm
Radial clearance	25 micrometers	15 micrometers
Lubricant viscosity	0.01 Ns/m <sup>2</sup>	

Table 1.